Genomic characterization of a novel virus found in papillomatous lesions from a southern brown bandicoot (Isoodon obesulus) in Western Australia

Author(s): Bennett, Mark D. ; Woolford, Lucy ; Stevens, Hans ; Van Ranst, Marc ; Oldfield, Timothy ; Slaven, Michael ; O'Hara, Amanda J. ; Warren, Kristin S. ; Nicholls, Philip K.

Year: 2008

Source: Virology, vol. 376, iss. 1, pp. 173-182.

Official URL: http://dx.doi.org/10.1016/j.virol.2008.03.014

Genomic characterization of a novel virus found in papillomatous lesions from a southern brown bandicoot (*Isoodon obesulus*) in Western Australia.

Mark D. Bennett[a], Lucy Woolford[a], Hans Stevens[b], Marc Van Ranst[b], Timothy Oldfield[c], Michael Slaven[a], Amanda J. O'Hara[a], Kristin S. Warren[a] and Philip K. Nicholls[a].

[a]School of Veterinary and Biomedical Sciences, Murdoch University, Perth, Western Australia, 6150, Australia. m.bennett@murdoch.edu.au; l.woolford@murdoch.edu.au; m.slaven@murdoch.edu.au; a.ohara@murdoch.edu.au; k.warren@murdoch.edu.au; p.nicholls@murdoch.edu.au.

[b]Laboratory of Clinical and Epidemiological Virology, Department of Microbiology and Immunology, Rega Institute for Medical Research, University of Leuven, Minderbroedersstraat 10 B-3000, Leuven, Belgium. hans.stevens@uz.kuleuven.ac.be; marc.vanranst@uz.kuleuven.ac.be.

[c]Wattle Grove Veterinary Hospital, 791 Welshpool Road, Wattle Grove, Western Australia, 6107, Australia. wgvh@iinet.net.au.

Corresponding author: Mark D. Bennett. School of Veterinary and Biomedical Sciences, Murdoch University, South Street, Murdoch, Western Australia, 6150, Australia. Phone: +618 9360 2479. Fax: +618 9310 4144. Email: m.bennett@murdoch.edu.au.

ABSTRACT

The genome of a novel virus, tentatively named bandicoot papillomatosis carcinomatosis virus type 2 (BPCV2), obtained from multicentric papillomatous lesions from an adult male southern brown bandicoot (*Isoodon obesulus*) was sequenced in its entirety. BPCV2 had a circular double-stranded DNA genome consisting of 7277 bp and open reading frames encoding putative L1 and L2 structural proteins and putative large T antigen and small t antigen transforming proteins. These genomic features, intermediate between *Papillomaviridae* and *Polyomaviridae* are most similar to BPCV1, recently described from papillomas and carcinomas in the endangered western barred bandicoot (*Perameles bougainville*). This study also employed *in situ* hybridization to definitively demonstrate BPCV2 DNA within lesion biopsies. The discovery of BPCV2 provides evidence of virus-host co-speciation between BPCVs and marsupial bandicoots and has important implications for the phylogeny and taxonomy of circular double-stranded DNA viruses infecting vertebrates.

KEY WORDS

Peramelidae; Marsupial; *Isoodon obesulus*; Virus-host co-speciation; Papillomatosis; Bandicoot papillomatosis carcinomatosis virus type 2; *In situ* hybridization

INTRODUCTION

The southern brown bandicoot, *Isoodon obesulus* (Shaw, 1797), is an Australian peramelid marsupial species that inhabits areas of southern mainland Australia, Tasmania and also several islands off the southern coast of Australia. A sub-species, *Isoodon obesulus peninsulae* occurs on the northern tip of the Cape York Peninsula, Queensland, Australia (Braithwaite, 2002). *I. obesulus* is nocturnal, omnivorous and adults typically weigh 400 - 1600 g. In Western Australia, this species is commonly known as the 'quenda', the name given to *I. obesulus* by local indigenous Australians (Braithwaite, 2002).

An adult male *I. obesulus* in poor health was found at Lesmurdie, Western Australia (32° 00'S, 116° 02'E) in April 2007 and taken to Kanyana Wildlife Rehabilitation Centre. During initial examination, multifocal to coalescing irregular, raised, alopecic and erythematous plaques were observed over the skin of the flanks, face and limbs. Routine skin scraping was performed, but no ectoparasites or fungal pathogens were identified. Initial treatment performed at Kanyana Wildlife Rehabilitation Centre included weekly oral Ivomec® (Ivermectin, Merial) and Malaseb (miconazole nitrate and chlorhexidine gluconate, DVM) baths. During this treatment, the bandicoot's weight and level of activity increased. General improvement of the skin condition was noted at a follow up veterinary examination, but the raised plaques persisted.

BPCV1 was recently discovered in western barred bandicoots (*Perameles bougainville*) in association with papillomatous and carcinomatous epithelial lesions grossly similar to the lesions evident on the southern brown bandicoot (Woolford et al., 2007; Woolford et al., 2008). Significantly, BPCV1 had certain genomic characteristics typical of *Papillomaviridae* and other genomic features classically associated with *Polyomaviridae* (Woolford et al., 2007). The 7295 bp double-stranded, circular DNA genome of BPCV1 was similar in size to known papillomaviruses (PVs), and it encoded putative structural proteins with greatest nucleotide and amino acid sequence similarity to the L1 and L2 capsid proteins of established PV types (Woolford et al., 2007). The putative transforming protein-encoding open reading frames (ORFs), most similar to large T antigen (LTag) and small t antigen (stag) occurred on the opposite DNA strand to the structural protein-encoding ORFs: features characteristic of the *Polyomaviridae* (Woolford et al., 2007).

Formerly, PVs and polyomaviruses (PyVs) were classified within a single family, *Papovaviridae*, but the current taxonomic paradigm recognizes the distinct phylogenies of PVs and PyVs by classifying them separately at the family level (de Villiers et al., 2004; Howley and Lowy, 2007; Imperiale and Major, 2007). Theoretically, PVs and PyVs may have evolved from a common ancestor virus (Van Ranst et al., 1995), and the discovery of BPCV1 suggested that a third lineage descended from this theoretical ancestor virus may exist today (Woolford et al., 2007). Alternatively, BPCV1 may have arisen in more recent evolutionary history from a recombination event between a PV and a PyV (Woolford et al., 2007).

The discovery of BPCV2 provides context and a point of comparison with BPCV1 to better elucidate their evolutionary histories and also provides additional information on the genomic features of these novel circular double-stranded DNA viruses that appear to have co-speciated with Australian marsupial bandicoot hosts.

RESULTS

Clinical examination. The southern brown bandicoot was referred to the Murdoch University School of Veterinary and Biomedical Sciences and there, a clinical examination revealed numerous multifocal to coalescing flat alopecic skin plaques involving approximately 10-15% of the total skin surface area (Fig. 1A-C). These lesions were evident on the fore- and hindpaws, fore- and hindlegs, thorax, flanks, lips, chin and face. The claw of the left lateral digit was overgrown and deformed medially across the palmar aspect of the left forepaw (Fig. 1B). Low numbers of *Hepatozoon* sp. gamonts were seen in blood smears, but nonetheless, the bandicoot was in excellent body condition and appeared otherwise healthy.

Microscopy. Routine histopathology revealed locally extensive epidermal hyperplasia of the strata spinosum and granulosum, with moderate anisokaryosis and anisocytosis of keratinocytes. There were also mild multifocal neutrophilic infiltrates in the superficial dermis and epidermis and mild dermal oedema. Rare suprabasilar mitotic figures were detected, occasionally the cytoplasm of stratum spinosum keratinocytes appeared

vacuolated (koilocytosis) and there were fewer hair follicles than normal (Fig. 1D). No parasitic, bacterial or fungal infections were demonstrable using routine or special histochemical stains. No PV capsid antigens were detected using indirect immunohistochemistry on biopsies of *I. obesulus* papillomatous lesions, though the positive control tissue section from a canine oral papillomavirus-infected tissue stained strongly positive. No virions were visualized in the skin fragments processed for transmission electron microscopy studies, though neither were intranuclear inclusions identified by light microscopy of histopathology sections.

Restriction enzyme analysis. The restriction endonuclease *Kpn*I produced 1 band at ~7.3 kb. *Sal*1 did not cut the DNA sample at all. *Bgl*II cut the genome twice, but produced only 1 very strong band ~3.6 kb. *Eco*RI produced 2 bands at ~5.1 kb, ~2.2 kb; *Bam*HI produced 3 fragments, ~5.1 kb, ~2.1 kb, and ~0.1 kb; and *Hin*dIII produced 6 bands ~3.4 kb, ~1.7 kb, ~ 1 kb, ~0.7 kb, ~0.3 kb and ~0.1 kb.

Polymerase chain reaction. The degenerate FAP59/64 primer pair (Forslund et al., 1999) successfully produced an amplicon of ~450 bp. Three primers specifically designed to amplify segments of the BPCV1 genome were used to amplify segments of the current isolate. The L1, L2r and stag primer pairs amplified products of the expected size. All other primer pairs failed to amplify DNA from the *I. obesulus* virus isolate, but did successfully amplify DNA from BPCV1 positive control samples. Genetic sequencing of the PCR amplicons obtained using the FAP59/64, L1, L2r and stag primer

pairs revealed 80%, 79%, 75% and 91% sequence similarity to the corresponding regions of the BPCV1 genome respectively.

Archived material. Photographs of gross lesions and a haematoxylin and eosin stained histological slide of the skin lesions have been deposited at the Australian Registry of Wildlife Health, Taronga Zoo, Mosman, NSW, Australia, ARWH No. 5925/1. The nucleotide sequence data reported here were archived in GenBank, National Center for Biotechnology Information under accession number **EU277647**.

Analysis of BPCV2 complete genomic sequence and deduced amino acid sequences. The genome of BPCV2 was a single circular molecule of double-stranded DNA that comprised 7277 bp and had a GC content of 37.52%. ORF analysis and BLASTX searches predicted the presence of 2 classical PV-like structural protein ORFs and 2 classical PyV-like transforming protein ORFs. The transforming-protein ORFs overlapped and were encoded on the opposite strand to the structural protein ORFs (Fig 2).

Non-coding regions. Between nt 1 and 840 was a non-coding region that contained putative TATA box sequences, T antigen binding sites (GAGGC), and a candidate site for the origin of DNA replication. This non-coding region corresponded with a similar non-coding region (79.6% aligned nucleotide identity) in the BPCV1 genome.

After alignment with BPCV1, a conserved TATA box sequence was detected ~40 bp upstream of the start codon of the *L2* ORF. A conserved T antigen binding site was found ~90 bp upstream of the *L2* ORF start codon but was encoded on the opposite DNA strand. Similarly, conserved TATA box sequences were detected ~50-60 bp 5' of the shared start codon of the *T antigen* ORFs. An A/T-rich imperfectly conserved nearly palindromic sequence (AGCCATTTTTTTTTTT(C/T)(A/C)GGCT) was found just near this TATA box sequence and is a candidate site for the origin of DNA replication.

Between the termination codons of the *L1* and *LTag* ORFs was a second 1276 bp non-coding region. There was a conserved potential T antigen binding motif identified within this region of the genome. BPCV2 and BPCV1 showed the lowest degree of aligned sequence identity (73.9%) in this region on a nucleotide basis.

A short 12 bp non-coding region was found between nt position 2251 and 2262 of the BPCV2 genome, separating the *L2* and *L1* ORFs.

The *L2* open reading frame. An ORF was identified between nt 841 and 2250 demonstrating greatest similarity to the *L2* ORF of BPCV1 (77.4% identity based on nucleotide sequence alignment). The translated sequence predicted a polypeptide consisting of 469 amino acid residues with a calculated molecular mass of 51.14 kDa and a theoretical isoelectric point at pH 4.87. The amino acid sequence was most similar to the L2 protein of BPCV1 (76.8% identity based on pairwise alignment of amino acid residues), but showed scant similarity to that of PV types (14-27%) (Table 1). Both

BPCVs had a potential furin cleavage site: RKKR between residues 5 and 8 of their L2 proteins.

The *L1* open reading frame. An ORF encoding a putative protein with greatest similarity to the L1 major capsid protein of a range of PV types was found between nt 2263 and 3771. This *L1* ORF was encoded on the same strand and in the same frame as the *L2* ORF. Nucleotide sequence similarity analysis revealed the *L1* ORF of BPCV2 was most similar to the BPCV1 *L1* ORF (81.2% aligned nucleotide identity). Translation of the nucleotide sequence yielded a predicted polypeptide containing 502 amino acid residues, with a molecular mass of 57.46 kDa and a theoretical isoelectric point at pH 7.04. The deduced amino acid sequence was most similar to the L1 protein predicted for BPCV1 with aligned amino acid identities of 88.5%, followed by β-PV types (57%) and PV types within other genera (40-50%) (Table 1). Both BPCVs retain highly conserved cysteine residues that in the putative L1 protein of BPCV2 are C-175, C-185 and C-431. The carboxy-terminal regions of both BPCVs' L1 proteins contain clusters of the basic amino acid residues lysine and arginine.

The *Large T antigen* open reading frame. Encoded on the opposite strand to the *L1* and *L2* ORFs and situated between nt 5049 and 7277 was an ORF encoding a protein similar to the LTags of PyVs. The predicted amino acid sequence consisted of <741 residues in a polypeptide with a molecular mass of <84.16 kDa and an isoelectric point at approximately pH 6.13. An intron that splices out the termination codon found after amino acid residue 225 was predicted, however due to the novelty of the BPCV1 and

BPCV2 sequences, the precise position of the splice donor and acceptor sites could not be confidently estimated. BPCV2 LTag showed greatest aligned amino acid sequence identity with BPCV1 LTag (87.2%), followed by the LTags of avian PyVs (32-35%) and eutherians PyVs (22-25%) (Table 1).

A DnaJ motif was found between amino acid residues 36-41: HPDKGG and a retinoblastoma protein binding motif (DLXCXE) was detected between residues 77 and 82: DLFCYE.

A possible nuclear localization signal: TPPKNK was found in the BPCV2 and BPCV1 LTags and similar motifs can be found in all PyV LTags except budgerigar fledgling disease virus (Pipas, 1992). In the LTag putative DNA binding region (Pipas, 1992), three amino acids were perfectly conserved across the BPCV, avian and eutherian PyV LTags. In BPCV2, these were: K-287, L-290 and R-325.

A zinc finger domain motif was present between residues 416-437: CKLCVKDQLLLTGLHKNHAKDH (Table 2). Following the zinc finger domain was a series of amino acid residues that were absolutely conserved among all PyVs and the BPCVs. In BPCV2, these were: N-443 A-444 Q-453 K-454 C-457 A-460 A-466 R-477 and R-484. A putative ATPase domain was found between residues 543-550: GPVNTGKT. Following this sequence there was a region in which 30 amino acid residues were perfectly conserved across all PyV and BPCV LTags. In the LTag from BPCV2, these were: A-553, E-577, L-578, L-602, G-605, G-607, N-610, L-611, D-612,

R-615, G-620, V-624, N-625, L-626, E-627, K-629, H-630, N-632, K-633, Q-636, F-638, P-639, P-640, T-644, N-646, Y-648, P-651, T-653, R-657 and R-684.

The *small t antigen* open reading frame. On the same strand and in the same frame as the *LTag* ORF, overlapping it between nt positions 6600 and 7277 of the BPCV2 genome was an ORF that encoded a putative polypeptide containing 225 amino acid residues. This predicted polypeptide had a calculated molecular mass of 25.87 kDa and a theoretical isoelectric point at pH 4.94. It included the DnaJ motif and retinoblastoma protein binding motif described above. Comparison of the aligned amino acid sequences revealed 87.1% identity with the BPCV1 stag, 17-21% identity with avian PyV stags and 10-15% identity with eutherian PyV stags (Table 1).

Phylogenetic analysis. A neighbour-joining phylogenetic tree was constructed based on the aligned nucleotide sequences of the *LTag* ORF of 13 members of the *Polyomaviridae*, BPCV1 and BPCV2. The tree had three main branches, one each for the PyVs of avians and eutherian mammals and another for BPCV1 and BPCV2 (Fig. 3).

A neighbour-joining phylogenetic tree was also constructed based on the aligned L1 encoding ORFs of 53 members of the *Papillomaviridae*, BPCV1 and BPCV2. In this L1 tree the PVs clustered in the previously defined genera, and high bootstrap values supported the nodes joining different PVs that belonged to the same genus. According to this tree, BPCV2 and BPCV1 were most closely related to the *Betapapillomavirus* genus,

but they branched off very close to the root of the common branch of this genus. Also, this clustering of the BPCVs was only supported by a low bootstrap value (56%) (Fig. 4).

Estimated time since divergence. Based upon the nucleotide sequence differences between the BPCV1 and BPCV2 *L1* ORFs (274 nucleotide substitutions over a 1462 bp unambiguously aligned region), these two viruses were estimated to have diverged from a common ancestor virus approximately 10.2 million years ago (mya) (95% confidence interval 8.0 – 14.8 mya). The same estimates were derived from calculations that included 3 in-frame codon deletion mutations in BPCV2 (285 nucleotide substitutions in a 1518 bp alignment). Calculations for the aligned *L2* ORFs (319 nucleotide substitutions over the entire 1410 bp *L2* ORF) yielded a similar result: divergence was estimated to have occurred 10.6 mya (95% confidence interval 8.2 – 15.5 mya).

Detection of BPCV2 using *in situ* hybridization. Strong positive staining of the nuclei of keratinocytes within papillomatous plaques was demonstrated using all 3 sub-ORF DNA probes and the genomic probe as well (Fig. 5A-D). Staining was limited to the nuclei of keratinocytes within the biopsied lesions and did not involve any cells within the dermis or subcutis. There was intense and frequent staining of keratinocytes within the stratum basale and stratum spinosum with less staining in the stratum granulosum, however staining of nuclei within all 3 of these layers was possible. RNase pretreatment did not demonstrably affect staining location, frequency or intensity (Fig. 5E). When DNA probes designed to anneal with BPCV1 DNA sequences were applied to southern brown bandicoot papillomatous lesion sections, no positive staining was achieved

(Bennett et al., 2008). Unexpectedly, when DNA probes designed to anneal with BPCV2 were applied to western barred bandicoot papillomatous lesion sections, some positive nuclear staining of keratinocytes resulted (Fig. 5F).

DISCUSSION

The negative results obtained using immunohistochemistry and electron microscopy were potentially misleading. Immunohistochemistry was only successful with papillomatous lesions from *P. bougainville* conjunctiva containing keratinocytes with intranuclear inclusion bodies (Woolford et al., 2008). Similarly, crystalline arrays of BPCV1 virions were demonstrated only in samples from *P. bougainville* conjunctiva with keratinocyte intranuclear inclusions (Woolford et al., 2008). Virions can only be visualized or immunohistochemically detected in mature lesions in which the late structural proteins have been expressed (Nicholls et al., 2001), therefore negative immunohistochemistry and transmission electron microscopy results do not preclude a viral aetiology.

The preliminary PCR and restriction enzyme results indicated that the current isolate was similar but not identical to BPCV1. BPCV1 had a circular double-stranded DNA genome consisting of 7295 bp (Woolford et al., 2007) while BPCV2 was only 18 bp shorter. The restriction enzyme digestion patterns of the two BPCVs differed, but they shared an identical and quite remarkable genomic organization (Woolford et al., 2007).

Papillomavirus genomes typically consist of ~8 kb and encode a series of early proteins followed by two late proteins and all these ORFs occur on one strand only (Howley and

Lowy, 2007). The BPCVs have no evidence of PV-like early protein nucleotide sequences, nor do they have E1 and E2 binding sequences near their putative origins of DNA replication.

Polyomavirus genomes are generally ~5 kb and have ORFs encoding structural proteins on one strand and transforming proteins on the opposite strand (Imperiale and Major, 2007). BPCV1 and BPCV2 do not have any nucleotide sequence similarity to the structural proteins of known PyVs however, both BPCVs encode putative transforming proteins with close similarities to the LTags and stags of PyVs (Woolford et al., 2007). There is a quite well conserved sequence that may act as an origin of DNA replication that has the general formula $AGCC(A/T/C)_{14}GGCT$ and is quite different from the origin of replication identified for avian PyVs: $TCC(A/T)_6GGA$ (Johne et al., 2006; Luo et al., 1994). After more BPCVs have been sequenced, if any exist, the importance of conserved motifs within the first non-coding region may become clearer.

There are several conserved motifs found in the amino acid sequences of BPCV1 and BPCV2 putative structural proteins which may be of functional significance. These include the possible furin cleavage site within the putative L2 proteins of BPCV1 and BPCV2 which may be necessary for endosome escape and intracellular trafficking of the virus genome (Richards et al., 2006); the highly conserved cysteine residues in the putative L1 proteins of the BPCVs that are thought to be important in dimerization and trimerization of the L1 major capsid protein of PVs (Ishii et al., 2003); and the clustering of basic amino acids such as lysine and arginine at the carboxyl terminus of the putative

L1 proteins of BPCV1 and BPCV2 which may facilitate interaction with negatively charged polysaccharides such as heparin and cell surface glycosaminoglycans (Joyce et al., 1999).

Similarly, the putative transforming proteins encoded by both BPCVs have conserved motifs that are likely to be important in understanding the pathogenesis of the diseases associated with these viruses at the molecular level. These include the DnaJ domain and the retinoblastoma binding region of stags and LTags which are thought to be important in mediating the displacement of E2F from its binding site on retinoblastoma proteins (pRb). Thus it appears likely that BPCV stags and the amino-terminal part of BPCV LTags displace pRb-bound E2F, which then activates promoters and stimulates entry into the cell cycle (Sheng et al., 1997). BPCV2, BPCV1 and all sequenced PyVs have a $CX_2CX_nHX_3H$ zinc finger motif which is thought to play a role in LTag oligomerization (Pipas, 1992). The ATPase domain is the most highly conserved region of PyV LTags and has the consensus sequence GP(V/I)(N/D)XGKT (Pipas, 1992). The ATPase domain is followed by 30 perfectly conserved amino acid residues may contribute to ATPase activity, p53 binding and LTag oligomerization (Pipas, 1992).

The *in situ* hybridization results demonstrated that both the PV-like and PyV-like parts of the BPCV2 genome could be found within the nuclei of keratinocytes of cutaneous papillomatous lesions of the affected southern brown bandicoot. This not only strengthens the association between the clinically apparent papillomatous lesions and BPVC2, but also supports the validity of the sequenced genome. Interestingly, BPCV1 is

known to infect both keratinocytes and sebocytes (Bennett et al., 2008), and a similar predilection pattern for BPCV2 cannot yet be excluded.

It is interesting that DNA probes designed to detect BPCV1 produced positive results only in *P. bougainville* biopsies, while DNA probes designed to detect BPCV2 produced positive results in both *P. bougainville* and *I. obesulus* biopsies. This counter-intuitive lack of reciprocity may be due to slight differences in probe cocktail formulation, probe concentrations or probe labeling efficiency between the two DNA probe batches or perhaps differences in the degree of tissue fixation. It is conceivable that some western barred bandicoots might have simultaneous BPCV1 and BPCV2 infections. Even though somewhat limited by the apparently imperfect specificity of BPCV2 DNA probes, *in situ* hybridization is a reliable screening technique for BPCV1 and BPCV2 in formalin-fixed paraffin-embedded biopsy samples (Bennett et al., 2008).

The discovery of *Hepatozoon* sp. in blood smears was considered an incidental finding, unassociated with any clinical signs. The estimated prevalence of *Hepatozoon* sp. infection in *I. obesulus* from Perth, Western Australia was 48% by examination of stained blood smears and 58% by PCR of DNA extracted from blood in a recent survey (Wicks et al., 2006).

Mitochondrial DNA evidence suggests that the two extant genera within the family Peramelidae, *Isoodon* and *Perameles*, diverged from a common bandicoot ancestor approximately 10 mya (Nilsson et al., 2004). The divergence of the host genera from a

common ancestor appears to be approximately coincident with the divergence of the BPCVs affecting them. This observation is supportive of the concept of virus-host co-speciation in which both modern day hosts and viruses arose from common ancestors (Shadan and Villarreal, 1993). Virus-host co-speciation has been recently demonstrated for λ-PVs affecting geographically disparate mammal hosts within the family Felidae (Rector et al., 2007). If the evolutionary rates estimated for λ-PVs are truly applicable to BPCVs, then the genomic analysis of host-specific DNA viruses could be used to verify the phylogenies their hosts (Rector et al., 2007).

Fossil evidence from south-eastern Queensland, Australia suggests *Perameles bougainville*, *Perameles nasuta* and *Isoodon obesulus* were sympatric there, during the Pleistocene and radiocarbon dating indicates these fossils were deposited around 40,000 to 45,000 years ago (Price, 2004). During the last glacial maximum, sea levels were ~130 m lower than the present day and the Australian mainland was conjoined with Tasmania, New Guinea and other modern day islands in a continent known as 'Sahul' (Mulvaney and Kamminga, 1999). Therefore, it is certainly possible that viruses similar to the BPCVs may still exist today in bandicoots inhabiting mainland Australia, Tasmania, New Guinea and the islands dotted around their respective coastlines. With this insight into the evolutionary history of BPCV types 1 and 2 in conjunction with the prehistoric geography of Sahul, the occurrence of BPCV1 in western barred bandicoots living on Bernier Island, off the western coast of Western Australia is no longer surprising.

The discovery of BPCVs in Australian bandicoots suggests that further research should be undertaken regarding the other skin-associated viruses collected from Australian animals. Several novel virus isolates are currently attributed to *Papillomaviridae* that were detected in Australian animals using PCR of swabs taken from non-lesional skin of koalas (*Phascolarctos cinereus*), eastern grey kangaroos (*Macropus giganteus*) and an echidna (*Tachyglossus aculeatus*) (Antonsson and McMillan, 2006). The PCR test employed the degenerate FAP59/64 primer pair which amplifies a ~450 bp region of the *L1* ORF of a wide range of PV types (Forslund et al., 1999; Antonsson and McMillan, 2006) but also successfully amplifies the *L1* region of BPCV1 and BPCV2 (Woolford et al., 2007). PV-like DNA was also found in a cutaneous papilloma in a possum (*Trichosurus vulpecula*) using PCR primers designed to anneal with the *L1* region of a range of PV types (Perrott et al., 2000). Clearly, these virus types could potentially be similar to the BPCVs were their genomes to be completely sequenced. Henceforth, sequence data derived solely from the *L1* ORF of novel virus isolates should be considered insufficient to attribute them to *Papillomaviridae*.

It has been theorized that modern day PVs and PyVs evolved from a common ancestor virus (Van Ranst et al., 1995), and if that is truly the case, it is possible that the BPCVs represent a third lineage descendent from that ancestral virus. Alternatively, the BPCVs may have arisen from a recombination event involving an ancient PV and an ancient PyV. If the latter hypothesis is correct, then it would seem that the recombination event took place more than ~10 mya, when Australia was physically isolated from all other continents on earth. Further analysis of viruses already isolated from the skin of various

marsupials and monotremes, and the possible discovery of more BPCV types from other bandicoot species may help to confirm which of these hypotheses is the more likely.

As it stands, the current virus taxonomic paradigm does not comfortably accommodate the BPCVs whose genomic features are intermediate between *Papillomaviridae* and *Polyomaviridae.* It is clear that the BPCVs are demonstrably and distinctly different to both PyVs and PVs and as such, their taxonomic position is presently undefined.

MATERIALS AND METHODS

Clinical examination and sample collection. The southern brown bandicoot was anesthetized with isoflurane (Isorrane, Baxter Healthcare) delivered by mask. Surgical sites were prepared aseptically and a 5 mm circular biopsy instrument was used to collect three skin samples. Skin wounds were closed with topical skin adhesive (Dermabond®, Ethicon) and 0.05 mL penicillin (Norocillin LA, Norbrook Laboratories) was administered subcutaneously. A small volume of blood was collected into an EDTA tube (Microtainer®, Becton-Dickinson) from the lateral tail vein using a 22 gauge needle and promptly used to make blood smears.

Sample processing. Smears were air dried and then stained with Wrights-Giemsa, mounted and examined with an Olympus BX-50 light microscope. Skin biopsy material was fixed for 4 hours in 10% neutral buffered formalin and then routinely processed using a Leica EG 1150C automatic processor (Leica Microsystems) before embedding in

paraffin wax. Blocks were sectioned at 5 μm with a Leica 2135 microtome (Leica Microsystems) and placed on silanised glass microscope slides (ProSciTech).

Histopathology. Slides were stained with Harris' haematoxylin and 1% eosin, Gram Twort to demonstrate bacteria or Periodic Acid Schiff's method to demonstrate fungi.

Indirect immunohistochemistry. A slide was dewaxed and rehydrated, then subjected to antigen retrieval using tris-EDTA buffer pH 9 and heated in a microwave (Kambrook, model: KER-686LE, 1150W) for four cycles of four minutes, twice on the reheat and twice on the low power setting. Endogenous peroxidase activity was blocked using 3% hydrogen peroxide and non-specific antibody binding was blocked with serum-free protein blocking agent (DakoCytomation). Rabbit polyclonal anti-bovine papillomavirus type 1 antibody (DakoCytomation) was diluted 1:600 with antibody diluent (DakoCytomation) and applied to tissue sections for 30 minutes, and rinsed thoroughly with phosphate buffered saline (PBS). Primary antibody binding was detected using the Envision^{+} R System Polymer-horseradish peroxidase (HRP) anti-rabbit secondary antibody solution (DakoCytomation) applied to sections for 30 minutes and washed thoroughly with PBS. Sections were then incubated in HRP substrate solution (DakoCytomation) for 3 minutes and rinsed in tap water and the slide was counterstained lightly with Harris' haematoxylin. Positive control tissue was obtained from a canine oral papilloma and this was subjected to the same conditions described above. A negative control slide was produced which simply omitted the addition of the primary antibody.

Transmission electron microscopy. Several 1-2 mm^3 pieces of papillomatous skin were fixed in 5% glutaraldehyde at 4 °C overnight. The pieces were washed in Sorensen's phosphate buffer and post-fixed in Dalton's chrome osmic acid, dehydrated through graded alcohols, transferred into propylene oxide, propylene oxide/Epon 812 and embedded in pure Epon 812 (TAAB Laboratories Equipment). Blocks had ultra thin sections cut, mounted on grids and stained with lead citrate and uranyl acetate. The grids were examined using a BioTwin CM 100 transmission electron microscope (Philips, Eindhoven, Holland) at an accelerating voltage of 80 kV.

DNA extraction and virus genome amplification. Total DNA was extracted from 25 mg of finely minced papillomatous skin biopsy material using the DNeasy Tissue Kit (Qiagen) according to the manufacturer's protocol. Multiply primed rolling circle amplification (RCA) was performed using the TempliPhi™ 100 Amplification Kit (Amersham Biosciences) on a 1 μL aliquot of the extracted DNA using a modified manufacturer's protocol (Rector et al., 2004; Woolford et al., 2007). The DNA concentration was quantified using a NanoDrop ND-1000 spectrophotometer (NanoDrop Technologies Inc.).

Restriction enzyme analysis. Six 2 μl aliquots of the RCA product were digested with 10 units of *Bam*HI, *Sal*I, *Hin*dIII, *Eco*RI, *Bgl*II or *Kpn*I (Promega) in a total volume of 20 μl for 8 hours at 37 °C. Following digestion, 15 μl of each digest reaction was subjected to gel electrophoresis in a 1% agarose gel laced with ethidium bromide. The resulting bands were visualized on a UV transilluminator.

PCR testing. Seven specific PCR primer pairs designed to amplify DNA within four identified ORFs, *L1*, *L2*, *stag* and *LTag* of the BPCV1 genome as well as degenerate FAP59/64 papillomavirus primers (Forslund et al., 1999) were used to screen the RCA product (Table 3). PCR reactions were carried out in a total volume of 40 μL with the following final concentrations of reagents 200 μmol/L each dNTP, 1× PCR reaction buffer, 1.0 mmol/L $MgCl_2$ pH 8.5, 200 nmol/L of each primer and 3.75 U/mL *Taq* DNA polymerase with 2 μL of 1:50 dilution of RCA product. This mixture was subjected to 95 °C for 3 minutes, then 25 cycles of 30 seconds at 95 °C, 30 seconds at 55 °C and 45 seconds at 72 °C, followed by 7 minutes at 72 °C in an automated thermocycler (Perkin Elmer Gene Amp PCR System 2400). The success of the reaction was checked by visualizing amplicons in a 1% agarose gel laced with ethidium bromide, electrophoresed at 90 V for 45 minutes and viewed on a UV transilluminator. PCR products were purified using the QIAquick® PCR purification kit (Qiagen) and DNA concentration determined using a NanoDrop ND-1000 spectrophotometer (NanoDrop Technologies Inc.).

DNA cloning and transformation. The BPCV2 genome, amplified by RCA was cut using *Kpn*I (which had only 1 recognition site in the *L2* ORF of the BPCV2 genome). A 1 μg quantity of pGEM 3f(+) DNA (Applied Biosystems) was linearized and dephosphorylated, then purified. The BPCV2 genome was cloned into the prepared pGEM 3f(+) plasmid using the Roche Rapid DNA ligation kit (Roche Diagnostics) according to the manufacturer's recommendations and immediately transformed into competent *Escherichia coli* (Invitrogen, One Shot MAX Efficiency DH5α-T1). The cells

were spread onto LB-ampicillin agar plates treated with X-gal, grown overnight and subjected to blue/white colony screening. Twelve white colonies were selected and screened using PCR for the virus genome insert. Insert-containing colonies were inoculated into ampicillin-treated LB broth cultures. Plasmids were prepared from the *E. coli* broth cultures using the QIAprep Spin Miniprep Kit (Qiagen) following the manufacturer's instructions and screened by PCR using the stag primer pair (Table 3) as well as *Kpn*I restriction digestion of the purified plasmids.

Plasmid sequencing. Three independent plasmid preparations were selected and further purified by ethanol precipitation. Sequencing of the purified plasmid DNA was performed in triplicate for each of the two strands of the 3 plasmid preparations with the Big Dye version 3.1 terminator kit (Applied Biosystems) using the dideoxynucleotide chain termination method (Sanger et al., 1977). The sequence was determined using an ABI Prism Applied Biosystems 377 automatic DNA sequencer (Applied Biosystems) at the State Agriculture and Biotechnology Centre, Perth, Western Australia. Chromatogram sequencing files were edited using Chromas Lite version 2.0 (Technelysium Pty. Ltd.) and the sequences aligned in BioEdit v.7.0.9.0 (Hall, 1999).

Nucleotide and protein sequence analysis. Putative ORFs were predicted using the National Center for Biotechnology Information (NCBI) online ORF Finder application (http://www.ncbi.nlm.nih.gov/gorf/gorf.html). The online Basic Local Alignment Search Tool (BLAST) was used to search GenBank for similar archived nucleotide and amino acid sequences. Identified ORF nucleotide sequences were translated using the online

Expasy Translate tool and the theoretical isoelectric point and molecular mass were estimated using the online Compute pI/Mw tool (http://www.expasy.ch/tools). Pairwise sequence identity scores were determined for BPCV2 and BPCV1 nucleotide and amino acid sequences after alignment using the ClustalW function within the BioEdit software (Hall, 1999). The same protocol was repeated with the appropriate sections of 16 PyV genomes (the avian PyVs CPyV [NC_007922], GHPyV [NC_004800], BFDV [NC_004764] and FPyV [NC_007923]; and the eutherian PyVs LPyV [NC_004763], WUV [NC_009539], JCV [NC_001699], HaPyV [NC_001663], BKV [NC_001538], Sa12 [NC_007611], BPyV [NC_001442], KIV [NC_009238], MPyV [NC_001515], MPnV [NC_001505], SquiPyV [NC_009951] and SV40 [NC_001669]) and 16 PV types (α-PVs HPV6b [NC_001355] and HPV16 [NC_001526]; β-PVs HPV5 [NC_001531] and HPV92 [NC_004500]; δ-PV BPV1 [NC_001522]; ζ-PV EcPV [NC_003748]; η-PV FcPV [NC_004068]; θ-PV PePV [NC_003973]; ι-PV MnPV [NC_001605]; κ-PV CRPV [NC_001541]; λ-PV COPV [NC_001619]; μ-PV HPV1 [NC_001356]; ν-PV HPV41 [NC_001354]; ξ-PV BPV3 [NC_004197]; o-PV PsPV [NC_003348]; and σ-PV EdPV1 [NC_006951]).

Phylogenetic analysis. Nucleotide sequences of the *L1* ORF of BPCV2 and BPCV1 and 53 PV-types were imported into the DAMBE software package version 4.2.13 and aligned at the amino acid level using ClustalW (Thompson et al., 1994; Xia and Xie, 2001). Subsequently, the corresponding nucleotide sequences were aligned, using the aligned amino acid sequences as a template. The nucleotide alignment was corrected manually in the GeneDoc Multiple Sequence Alignment Editor and Shading Utility

software package version 2.6.003 (Nicholas et al., 1997) and only the unambiguously aligned parts of the *L1* ORF were used in the phylogenetic analysis. Based on this alignment, a phylogenetic tree was constructed using the neighbour-joining method in MEGA version 3.1 (Kumar et al., 2004). Bootstrap support values were obtained for 10,000 replicates.

For the *LTag* of BPCV2, the evolutionary relationship to BPCV1 and 13 PyVs was investigated. The predicted intron sequence within the BPCV2 *LTag* ORF could not be confidently identified therefore the analysis was performed on the complete *LTag* ORFs, including intron sequences. The *LTag* nucleotide sequences were aligned with the ClustalW algorithm using DAMBE (Thompson et al., 1994; Xia and Xie, 2001). The Gblocks computer program version 0.91b was used to remove the divergent regions and positions in which the sequences were ambiguously aligned (Castresana, 2000). Based on this corrected alignment, a neighbour-joining phylogenetic tree was constructed in the same way as described above.

Estimated time since divergence. The calculations for estimating the time since BPCV1 and BPCV2 diverged from a theoretical common ancestor virus were based on the average mutation rates and associated 95% confidence intervals determined for the *L1* and *L2* ORFs of λ-PVs affecting hosts within Felidae (Rector et al., 2007). The mutation rate estimates were: *L1* 1.84×10^{-8} ($1.27 \times 10^{-8} – 2.35 \times 10^{-8}$); and *L2* 2.13×10^{-8} ($1.46 \times 10^{-8} – 2.76 \times 10^{-8}$) nucleotide substitutions per site per year (Rector et al., 2007).

Generation of genomic digoxigenin-labeled DNA probes for *in situ* hybridization. Genomic DNA probes were generated using nick translation (Roche Diagnostics) following a modified manufacturer's protocol (Bennett et al., 2008).

Generation of sub-ORF digoxigenin-labeled DNA probes for *in situ* hybridization. Amplicons within 3 ORFs of the BPCV2 genome, *L1*, *L2* and *stag* were obtained by PCR using the L1, L2r and stag primer pairs (Table 3). PCR products were purified using the QIAquick® PCR purification kit (Qiagen) and DNA concentration determined using a NanoDrop ND-1000 spectrophotometer (NanoDrop Technologies Inc.). Purified PCR product DNA was used to generate digoxigenin-labeled DNA probes by the nick translation method described in the manufacturer's protocol (Roche Diagnostics).

***In situ* hybridization.** The optimized *in situ* hybridization protocol developed for detecting BPCV1 DNA within skin biopsies from western barred bandicoots was precisely followed (Bennett et al., 2008).

ACKNOWLEDGMENTS

This project was funded by the Australian Research Council in partnership with Murdoch University and the Western Australian Department of Environment and Conservation (DEC) under Linkage Project LP0455050. The laboratory work and genome sequencing were conducted at the Western Australian State Agricultural Biotechnology Centre. We are grateful to the volunteers at Kanyana Wildlife Rehabilitation Centre for bringing this case of clinical papillomatosis in a southern brown bandicoot to our attention. Thanks

also to Frances Brigg for her helpful advice regarding DNA sequencing, Gerard Spoelstra for preparing the histopathology slides, Peter Fallon for his assistance with electron microscopy studies, Dr. Phillip Clark, and the Murdoch University Clinical Pathology Laboratory for help with blood smears.

REFERENCES

Antonsson, A., McMillan, A. J., 2006. Papillomavirus in healthy skin of Australian animals. J. Gen. Virol., 87, 3195-3200.

Bennett, M. D., Woolford, L., O'Hara, A. J., Warren, K. S., Nicholls, P. K., 2008. *In situ* hybridization to detect bandicoot papillomatosis carcinomatosis virus type 1 in biopsies from endangered western barred bandicoots (*Perameles bougainville*). J. Gen. Virol., 89, 419-423.

Braithwaite, R. W., 2002. Southern Brown Bandicoot. In: Strahan, R. (Ed.), The mammals of Australia 2nd edition. Reed New Holland, Frenchs Forest, New South Wales, pp. 176-177.

Castresana, J., 2000. Selection of conserved blocks from multiple alignments for their use in phylogenetic analysis. Mol. Biol. Evol., 17, 540-552.

de Villiers, E., Fauquet, C., Broker, T. R., Bernard, H., zur Hausen, H., 2004. Classification of papillomaviruses. Virology, 324, 17-27.

Forslund, O., Antonsson, A., Nordin, P., Stenquist, B., Hansson, B. G., 1999. A broad range of human papillomavirus types detected with a general PCR method suitable for analysis of cutaneous tumours and normal skin. J. Gen. Virol., 80, 2437-2443.

Hall, T. A., 1999. BioEdit: a user-friendly biological sequence alignment editor and analysis program for Windows 95/98/NT. Nucleic Acids. Symp. Ser., 41, 95-98.

Howley P. M., Lowy, D. R., 2007. Papillomaviruses. In: Knipe, D. M., Howley P. M. (Eds.), Fields Virology 5th edition. Lippincott Williams and Wilkins, Philadelphia, PA, pp. 2299-2354.

Imperiale, M. J., Major, E. O., 2007. Polyomaviruses. In: Knipe, D. M., Howley P. M. (Eds.), Fields Virology 5th edition. Lippincott Williams and Wilkins, Philadelphia, PA, pp. 2263-2298.

Ishii, Y., Tanaka, K., Kanda, T., 2003. Mutational analysis of human papillomavirus type 16 major capsid protein L1: the cysteines affecting the intermolecular bonding and structure of the L1-capsids. Virology, 308, 128-136.

Johne, R., Wittig, W., Fernandez-de-Luco, D., Hofle, U., Muller, H., 2006. Characterization of two novel polyomaviruses of birds by using multiply primed rolling-circle amplification of their genomes. J. Virol., 80, 3523-3531.

Joyce, J. G., Tung, J-S., Przysiecki, C. T., Cook, J. C., Lehman, E. D., Sands, J. A., Jansen, K. U., Keller, P. M., 1999. The L1 major capsid protein of human papillomavirus type 11 recombinant virus-like particles interacts with heparin and cell-surface glycosaminoglycans on human keratinocytes. J. Biol. Chem., 274, 5810-5822.

Kumar S., Tamura, K., Nei, M., 2004. MEGA3: Integrated software for Molecular Evolutionary Genetics Analysis and sequence alignment. Briefings in Bioinformatics, 5, 150-163.

Luo, D., Muller, H., Tang, X. B., Hobom, H., 1994. Expression and DNA binding of budgerigar fledgling disease virus large T antigen. J. Gen. Virol., 75, 1267-1280.

Mulvaney, D. J., Kamminga, J., 1999. Prehistory of Australia, Allen and Unwin. St. Leonards, New South Wales.

Nicholas K. B., Nicholas, H. B., Deerfield, D. W., 1997. GeneDoc: analysis and visualization of genetic variation. Embnet. News., 4, 14.

Nicholls, P. K., Doorbar, J., Moore, R. A., Pei, W., Anderson, D. M., Stanley, M. A., 2001. Detection of viral DNA and E4 protein in basal keratinocytes of experimental canine oral papillomavirus lesions. Virology, 284, 82-98.

Nilsson, M. A., Arnason, U., Spencer, P. B. S., Janke, A., 2004. Marsupial relationships and a timeline for marsupial radiation in South Gondwana. Gene, 340, 189-196.

Perrott, M. R. F., Meers, J., Greening, G. E., Farmer, S. E., Lugton, I. W., Wilks, C. R., 2000. A new papillomavirus of possums (*Trichosurus vulpecula)* associated with typical wart-like lesions. Arch. Virol., 145, 1247-1255.

Pipas, J. M., 1992. Common and unique features of T antigens encoded by the polyomavirus group. J. Virol., 66, 3979-3985.

Price, G. J., 2004. Fossil bandicoots (Marsupialia, Peramelidae) and environmental change during the Pleistocene on the Darling Downs, southeastern Queensland, Australia. J. Syst. Palaentol., 2, 347-356.

Rector, A., Tachezy, R., Van Ranst, M., 2004. A sequence-independent strategy for detection and cloning of circular DNA virus genomes by using multiply primed rolling-circle amplification. J. Virol., 78, 4993-4998.

Rector, A., Lemey, P., Tachezy, R., Mostmans, S., Ghim, S-J., Van Doorslaer, K., Roelke, M., Bush, M., Montali, R. J., Joslin, J., Burk, R. D., Jenson, A. B., Sundberg, J. P., Shapiro, B., Van Ranst, M., 2007. Ancient papillomavirus-host co-speciation in Felidae. Genome Biol., 8, R57.

Richards, R. M., Lowy, D. R., Schiller, J. T., Day, P. M., 2006. Cleavage of the papillomavirus minor capsid protein, L2, at a furin consensus site is necessary for infection. Proc. Nat. Acad. Sci. USA., 103, 1522-1527.

Sanger, F., Nicklen, S., Coulson, A. R., 1977. DNA sequencing with chain-terminating inhibitors. Proc. Natl. Acad. Sci. USA., 74, 5463–5467.

Shadan, F. F., Villarreal, L. P., 1993. Coevolution of persistently infecting small DNA viruses and their hosts linked to host-interactive regulatory domains. Proc. Natl. Acad. Sci. USA., 90, 4117-4121.

Sheng, Q., Denis, D., Ratnofsky, M., Roberts, T. M., DeCaprio, J. A., Schaffhausen, B., 1997. The DnaJ domain of polyomavirus large T antigen is required to regulate Rb family tumor suppressor function. J. Virol., 71, 9410-9416.

Thompson J. D., Higgins, D. G., Gibson, T. J., 1994. CLUSTAL W: improving the sensitivity of progressive multiple sequence alignment through sequence weighting,

position-specific gap penalties and weight matrix choice. Nucleic Acids Res., 22, 4673-4680.

Van Ranst, M., Kaplan, J. B., Sundberg, J. P., Burk, R. D., 1995. Molecular evolution of papillomaviruses. In: Gibbs, A., Calister, C. H., Garcia-Arenal, F. (Eds.), Molecular basis of virus evolution. Cambridge University Press, Cambridge, pp. 455-476.

Wicks, R. M., Spencer, P. B. S., Moolhuijzen, P., Clark, P., 2006. Morphological and molecular characteristics of a species of *Hepatozoon* Miller, 1908 (Apicomplexa: Adeleorina) from the blood of *Isoodon obesulus* (Marsupialia: Peramelidae) in Western Australia. System. Parasitol., 65, 19-25.

Woolford, L., O'Hara, A. J., Bennett, M. D., Slaven, M., Swan, R., Friend, J. A., Ducki, A., Sims, C., Hill, S., Nicholls, P. K., Warren, K. S., 2008. Cutaneous papillomatosis and carcinomatosis in the western barred bandicoot (*Perameles bougainville*). Vet. Pathol., 45, 95-103.

Woolford, L., Rector, A., Van Ranst, M., Ducki, A., Bennett, M. D., Nicholls, P. K., Warren, K. S., Swan, R. A., Wilcox, G. E., O'Hara, A. J., 2007. A novel virus detected in papillomas and carcinomas of the endangered western barred bandicoot (*Perameles bougainville*) exhibits genomic features of both the *Papillomaviridae* and *Polyomaviridae*. J. Virol., 81, 13280-13290.

Xia, X., Xie, Z., 2001. DAMBE: software package for data analysis in molecular biology and evolution. J. Hered., 92, 371-373.

Table 1. Comparisons of aligned amino acid sequences from BPCV2 to BPCV1, polyomaviruses and selected papillomavirus types.

Type	LTag	stag	Type	Genus	L1	L2
BPCV1	87.2	87.1	BPCV1		88.5	76.8
CPyV[a]	35	19	HPV5	β	57	27
GHPyV[a]	34	21	HPV92	β	57	24
BFDV[a]	33	17	CRPV	κ	50	19
FPyV[a]	32	18	BPV3	ξ	49	27
LPyV[b]	25	15	COPV	λ	49	24
SquiPyV[b]	25	12	HPV1	μ	49	23
WUV[b]	24	14	HPV6b	α	49	22
JCV[b]	22	12	MnPV	ι	48	24
HaPyV[b]	22	12	EdPV	Σ	48	22
MPnV[b]	22	11	HPV16	α	46	23
BKV[b]	22	11	PsPV	ο	46	20
Sa12[b]	22	11	EcPV	ζ	45	21
BPyV[b]	22	11	BPV1	δ	45	19
KIV[b]	22	10	HPV41	N	44	21
MPyV[b]	20	13	PePV	θ	41	17
SV40[b]	20	11	FcPV	η	41	14

[a]Avian polyomaviruses

[b]Eutherian polyomaviruses

Table 2. Zinc finger motifs found in the Large T antigens of bandicoot papillomatosis carcinomatosis virus types 1 and 2 and polyomaviruses.

Virus	Large T antigen amino acid sequence
BPCV2	^{412}SPQG**C**KL**C**VKDQLLLTGLHKNHAKD**H**CKH**H**E^{442}
BPCV1	^{411}TIQG**C**KL**C**VKDQLLLTGLHKNHAKD**H**VQH**H**E^{441}
FPyV	^{290}PVEA**C**PD**C**AKERETAKRQRTS**H**LED**H**PAHQK^{306}
BFDV	^{254}PTDK**C**PE**C**QKDKDTVKRKRST**H**IDD**H**PRHQH^{284}
CPyV	^{294}NPDE**C**KD**C**KEDRENSSLQRLKRRRPGG**H**LED**H**ATH**H**M^{330}
GHPyV	^{290}PQEE**C**AD**C**QSQKENLCFGQLKRKWYGG**H**LDD**H**GIH**H**N^{326}
BKV	^{300}NVEE**C**KK**C**QKKDQPY**H**FKY**H**EKHFA^{324}
JCV	^{299}NPQQ**C**KK**C**EKKDQPN**H**FN**HH**EK**H**YY^{323}
SV40	^{298}SFEM**C**LK**C**IKKEQPS**H**YKY**H**EKHYA^{322}
SA12	^{300}NPEE**C**RK**C**QKKEQPY**H**FKF**H**EKHFA^{324}
LPV	^{363}EPGK**C**GK**C**EKKQHKF**H**YNY**H**KAH**H**A^{387}
HaPyV	^{422}CESS**C**KK**C**AEALPRMKV**H**WAN**H**SQHLE^{448}
PyV	^{448}EVPS**C**IK**C**SKEETRLQI**H**WKN**H**RKHAE^{474}
KIV	^{310}KPEE**C**EK**C**SKNDDAT**H**KRV**H**VQN**H**EN^{335}
WUV	^{317}KVEE**C**EK**C**NSNEDAT**H**NRL**H**MEHQK^{341}
BPyV	^{255}APEA**C**KV**C**DNPRRLE**H**RRH**H**T^{275}
MPnV	^{314}PVPN**C**SK**C**ENRMLTN**H**FKF**H**KEH**H**E^{338}
SquiPyV	^{307}NPST**C**SK**C**DQKVIVD**H**YKY**H**SLHYA^{331}

Table 3. PCR primer pairs used during the initial screening of the DNA amplified from papillomatous lesions from *Isoodon obesulus*.

Primer	Forward	Reverse	Size
L1	AGATTGGCGTTCCTAAGGTG	TCATCATCCCCTTCTTTTGC	250
LTag	TGCAAAGTCCGCTAAGGATT	TGTGGCGAATCATCTTTGTC	184
LTagr	GTTAATGGAATTCCTGATAGATTGCA	GAAATCTTTAGTAAAGGATCCAGAATAC	426
Stag	ATTCTGGATCCAGTGAGGGAA	CCCATAATTAACAGAATTCATCAGTGA	308
L2r	GGAACAAGAATTCTAAAACCTCCA	GCTTCTGGATCCATCAACCTA	647
L2	AAGGACAAAATTGAAGGAACCA	ACAGCATCAACTGGGAGGAT	236
L1r	GGTAATATGAATTCTAAAGCCCTTA	AGAATTCTAGGATCCATTGCATTTA	590
FAP59/64*	TAACWGTIGGICAYCCWTATT	CCWATATCWVHCATITCICCATC	450

*W = T/C; I = inosine; Y = C/T; V = A/C/G; H = A/C/T (Forslund et al., 1999)

Figure 1. A-C. Photographs of a 2 kg adult male southern brown bandicoot (*Isoodon obesulus*) affected by multicentric papillomatosis. The multifocal to coalescing red-black flat, alopecic plaques were found on the face (A), forelimbs (B), hindlimbs, thorax and abdomen (C). The claw of the lateral digit of the left forelimb (B) was elongated and had deviated medially to lie across the palmar aspect of the manus. (D) Photomicrograph of a haematoxylin and eosin stained slide of a skin biopsy from the southern brown bandicoot. There is mild orthokeratotic hyperkeratosis with a hyperplastic stratum basale. The strata spinosum and granulosum are hyperplastic and display anisocytosis, anisokaryosis and occasional suprabasilar mitoses (arrow). There is also a mild neutrophilic inflammatory infiltrate in the superficial dermis. Bar = 50 μm.

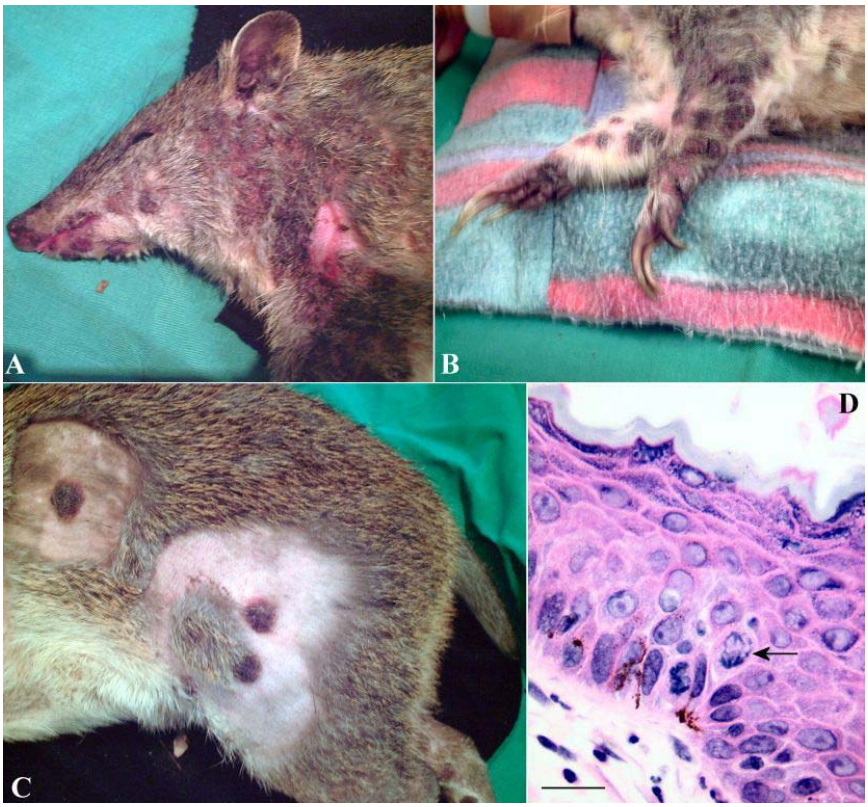

Figure 2. Genome map of bandicoot papillomatosis carcinomatosis virus type 2 (BPCV2).

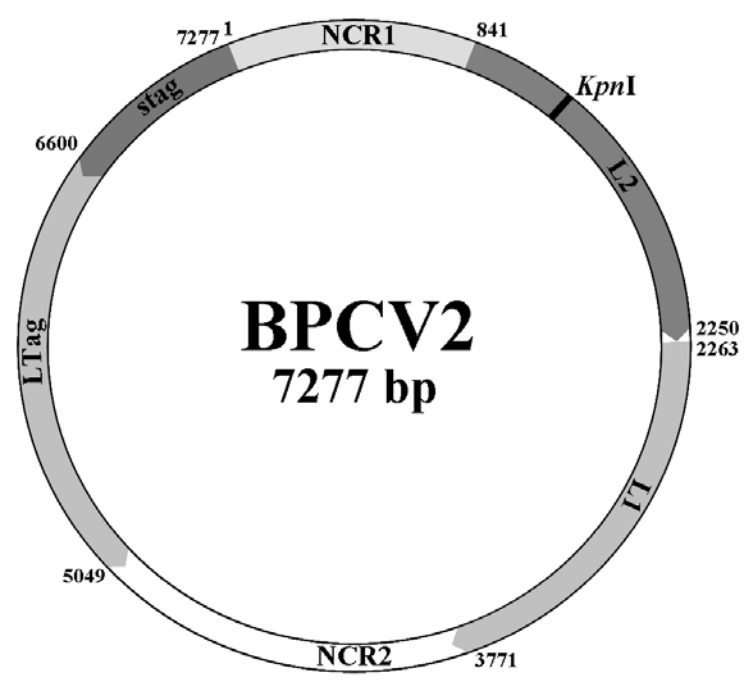

Figure 3. Large T antigen phylogenetic tree of BPCV2, BPCV1 and 13 established PyVs [LPyV (NC_004763), SV40 (NC_001669), Sa12 (NC_007611), HaPyV (NC_001663), MPyV (NC_001515), MPnV (NC_001505), BPyV (NC_001442), JCV (NC_001699), BKV (NC_001538), BFDV (NC_004764), GHPyV (NC_004800), CPyV (NC_007922), and FPyV (NC_007923)] showing the evolutionary relationship of the BPCV2 and BPCV1 sequences to members of the *Polyomaviridae*. Phylogenetic reconstruction was performed by the neighbour-joining method. Bootstrap percentages (based on 10,000 iterations) of ≥ 80% are shown at internal nodes and the genetic distance in nucleotide substitutions per site is indicated by the scale bar. The clusters of PyVs that infect avian and eutherian host species, respectively, are indicated.

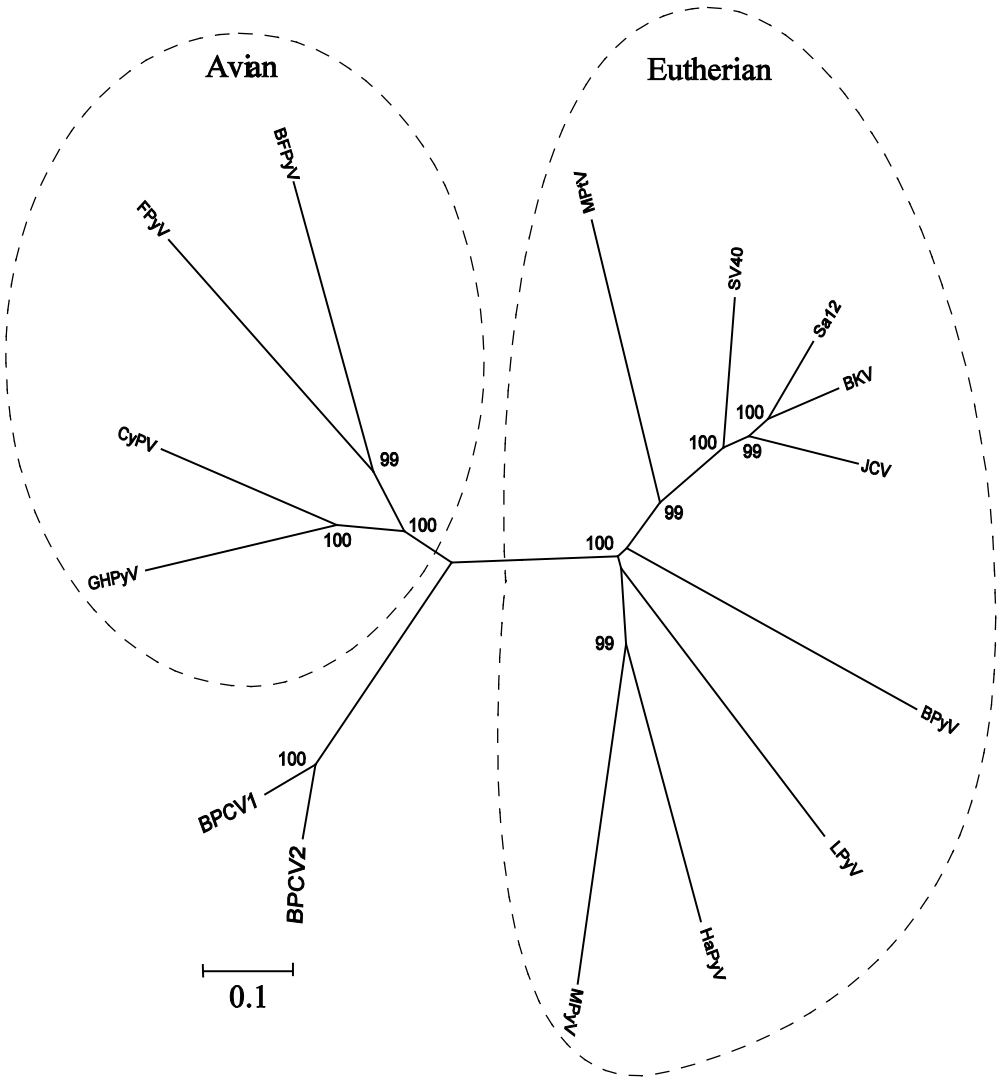

Figure 4. Evolutionary relationship of the BPCV2 and BPCV1 L1 sequences to members of the *Papillomaviridae*. Shown is a neighbour-joining phylogenetic tree of the L1 sequences of BPCV2, BPCV1 and 53 PVs [genus *Alphapapillomavirus*, HPV32 (NC_001586), HPV10 (NC_001576), HPV61 (NC_001694), HPV2 (NC_001352), HPV26 (NC_001583), HPV53 (NC_001593), HPV18 (NC_001357), HPV7 (NC_001595), HPV16 (NC_001526), HPV6 (NC_001355), HPV34 (NC_001587), RhPV1 (NC_001678), HPV54 (NC_001676), HPV90 (NC_004104), and HPV71 (AY330621); genus *Betapapillomavirus*, HPV5 (NC_001531), HPV9 (NC_001596),

HPV49 (NC_001591), HPV92 (NC_004500), and HPV96 (NC_005134); genus *Gammapapillomavirus*, HPV4 (NC_001457), HPV48 (NC_001690), HPV50 (NC_001691), and HPV60 (NC_001693); genus *Deltapapillomavirus*, EEPV (NC_001524), DPV (NC_001523), OvPV1 (NC_001789), and BPV1 (NC_001522); genus *Epsilonpapillomavirus*, BPV5 (NC_004195); genus *Zetapapillomavirus*, EcPV1 (NC_003748); genus *Etapapillomavirus*, FcPV (NC_004068); genus *Thetapapillomavirus*, PePV (NC_003973); genus *Iotapapillomavirus*, MnPV (NC_001605); genus *Kappapapillomavirus*, CRPV (NC_001541) and ROPV (NC_002232); genus *Lambdapapillomavirus*, canine oral PV (COPV) (NC_001619), FdPV1 (NC_004765), and *Procyon lotor* PV (NC_007150); genus *Mupapillomavirus*, HPV1 (NC_001356) and HPV63 (NC_001458); genus *Nupapillomavirus*, HPV41 (NC_001354); genus *Xipapillomavirus*, BPV3 (NC_004197); genus *Omicronpapillomavirus*, PsPV1 (NC_003348); genus *Pipapillomavirus*, HaOPV (E15111); genus *Rhopapillomavirus*, TmPV1 (NC_006563); genus *Sigmapapillomavirus*, EdPV1 (NC_006951); and unclassified types RaPV1 (NC_008298), BPV7 (NC_007612), CPV2 (NC_006564), CPV3 (NC_008297), ChPV1 (NC_008032), McPV2 (DQ664501) and MmPV (NC_008582)]. The established PV genera are indicated by their Greek symbols. The scale bar indicates the genetic distance (in nucleotide substitutions per site), and the numbers at the internal nodes represent the bootstrap probability percentages as determined for 10,000 iterations by the neighbour-joining method. Only bootstrap values of 80% or more are shown.

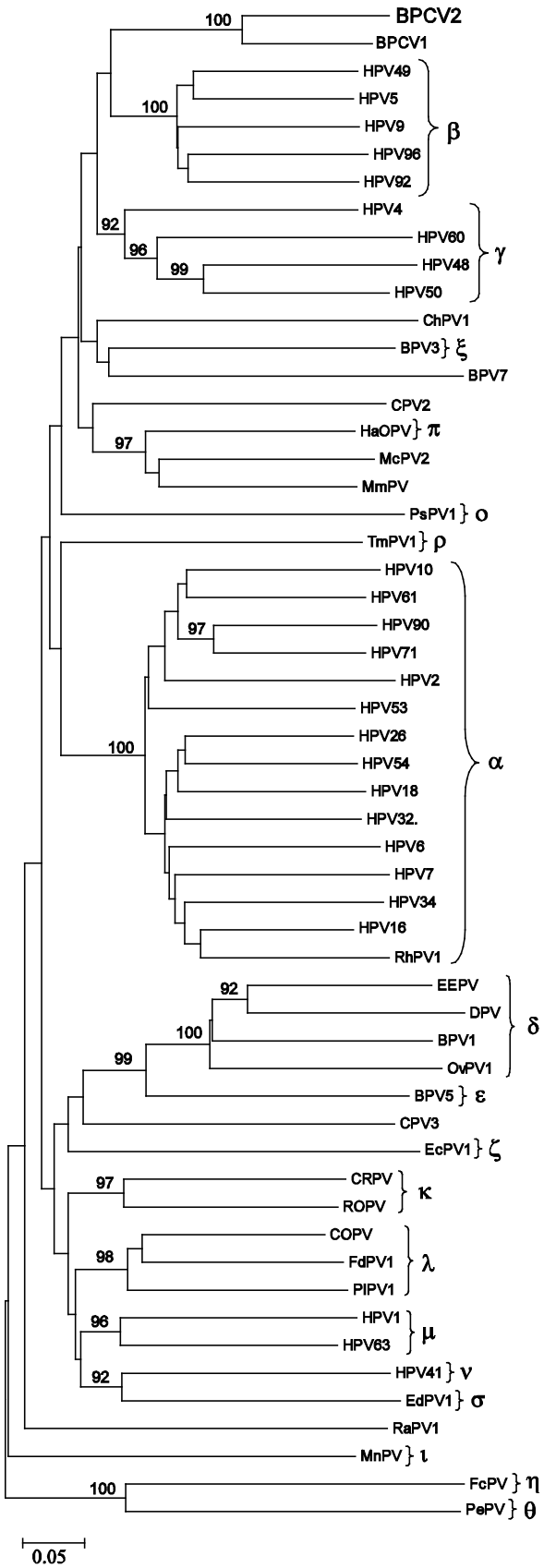
BPCV2
BPCV1
HPV49
HPV5
HPV9
HPV96
HPV92
β
HPV4
HPV60
HPV48
HPV50
γ
ChPV1
BPV3
ξ
BPV7
CPV2
HaOPV
π
McPV2
MmPV
PsPV1
ο
TmPV1
ρ
HPV10
HPV61
HPV90
HPV71
HPV2
HPV53
HPV26
HPV54
HPV18
HPV32.
HPV6
HPV7
HPV34
HPV16
RhPV1
α
EEPV
DPV
BPV1
OvPV1
δ
BPV5
ε
CPV3
EcPV1
ζ
CRPV
ROPV
κ
COPV
FdPV1
PlPV1
λ
HPV1
HPV63
μ
HPV41
ν
EdPV1
σ
RaPV1
MnPV
ι
FcPV
η
PePV
θ
100
92
100
92
96
99
97
100
92
100
99
97
98
96
92
100
0.05

Figure 5. *In situ* hybridizations. (A) BPCV2 genomic probe. (B) BPCV2 *L1* probe. (C) BPCV2 *L2* probe. (D) BPCV2 *stag* probe. (E) BPCV2 genomic probe applied after RNase pretreatment. (F) BPCV2 genomic probe applied to *P. bougainville* papillomatous lesions. Brazilin haematoxylin counter stain. Bar = 50 µm.